Bandwidth and Pattern Reconfigurable Antenna

A.Khalat

A.Khalat@sabu.edu.ly

Department of Electrical Engineering, Faculty of Engineering, Sabratha University, Libya

ABSTRACT

This paper presents a reconfigurable antenna (RA) capable of varying its impedance bandwidth between 3.4-3.6 GHz and 3.1-3.9 GHz frequency bands and steering its main beam into three different directions pertaining to $\theta \in \{-30^\circ, 0^\circ, 30^\circ\}$, $\varphi \in \{0^\circ\}$ for each band. The RA employs a multilayer structure, where two parasitically coupled reconfigurable layers using PIN diode switches enable generating the modes of operation. A fully functional RA has been fabricated and characterized. The characterizations involved impedance, radiation, error vector magnitude (EVM), and inter modulation (IM) measurements. An average realized gain of 9 dB has been achieved for all modes of operation. EVM measurements indicate less than -25dB EVM for input powers up to 30dBm. IM test results have revealed that the passive factors such as loose solder joints and electro-thermal effects are the main factors resulting in passive IM products.

Keywords: Aperture coupling, Yagi-Uda arrays, Reconfigurable antennas, Microstrip antennas, Multifrequency antennas, Frequency control

1. Introduction

Spectrum sharing has gained much attention in recent years due to the scarcity of available spectrum at lower frequency bands and the underutilization of licensed bands [1]–[5]. The goal is to enable secondary or tertiary users or devices to access the unused licensed spectrum provided that the primary users of the licensed bands are not harmfully interfered [5]–[7]. In general, wide band sensing capability is required to determine the available bands, where transmission is permitted. To that end, a wide band antenna for sensing the spectrum and a reconfigurable narrowband antenna (RA) with frequency tunability enabling communication on the available bands are needed. Typically, two separate antennas, a large size wide band antenna and a small size reconfigurable narrow band antenna, are integrated in the same platform [8]–[10].

While this technique offers both wide and narrow band operations, poor isolation between sensing and communication antennas due to limited available space can degrade system level performance. Therefore, a single RA with bandwidth reconfigurable property that can be used for both sensing and communication to improve isolation between sensing and communication would be advantageous [11]–[13].

The single RA element presented in this work is capable of performing both wide and narrow bandwidth operations. In addition, this RA can steer its main radiation beam towards three different directions for both bands. Combining bandwidth and pattern reconfigurability in a single

compact platform provides advantages in effective sensing, transmission and frequency reuse. This RA design consists of four layer structure with three reconfigurable layers and a driven antenna layer Radiation and impedance properties, i.e., reflection coefficient and radiation pattern, are most commonly used to characterize antennas. As the goal of using RAs in a transceiver system is to benefit the overall system level performances, characterization of the impacts that an RA plays on parameters such as Error Vector Magnitude (EVM), which is used as a measure to quantify the performance of a transceiver, becomes important. Also, signal distortion due to intermodulation (IM) products, whether it is passive IM (PIM) or is due to active elements, such as PIN diodes, need to be measured to properly represent the full impact of antenna characteristics on the system performance. Signal distortion measurements have commonly been focused on RF-frontend (RFFE). However tighter integration between RFFE and antennas, and increased use of various non-linear devices, such as PIN and varactor diodes, in antenna terminals makes the system vulnerable to non-linear distortions. Therefore, it is necessary to measure and minimize these distortions in antenna terminals to ensure high performance. For traditional non-reconfigurable antennas, there are some works that investigated EVM [14], [15] and passive inter modulation (PIM) [16], [17]. Number of non- linear devices integrated with multi-layer RAs warrant IM and EVM measurements to precisely determine the impacts that an RA plays on them. To that end, this work puts a great deal of efforts on characterizing the IM and EVM performances of the proposed RA. The main contributions of this work compared to similar other works can be summarized as follows, 1) concurrent configuration of impedance bandwidth and radiation pattern, 2) high average realized gain (~9dB) for all modes of operation in a relatively compact profile, and 3) system level performance investigation of the RA in terms of EVM and PIM.

2. Antenna Structure and Working Mechanism

2.1 Geometry of the Reconfigurable Antenna (RA)

The geometry of the RA, as shown in Fig. 1, consists of four main layers, namely feed, driven antenna (aperture coupled patch), parasitic patch and parasitic pixel layers. The aperture coupled patch, which has been described in various works [18]–[20], has been chosen for its relatively broad bandwidth and high degree of freedom in impedance tuning. The driven antenna couples EM energy to the parasitic patch and pixel layers, which are placed 6.096mm and 8.145mm above the driven patch layer, and formed with 1.52mm and 0.813mm thick RO400C substrates, respectively. Both of these layers are supported by four posts and the air layers underneath act as the main low loss medium (see Fig. 1). The upper surfaces of the parasitic patch and pixel layers consist of a grid of 3 ×3 and 3 × 2 metallic pixels, respectively. The adjacent rectangular metallic pixels in both parasitic patch and pixel layers are connected via PIN diode switches, as shown in the magnified sections of Fig. 1(a). A single PIN diode is also inserted in the microstrip feed line, as shown in the feed layer of Fig. 1(a), which enables to change the length of the microstrip line, thereby providing impedance matching. These PIN diodes are turned ON/OFF by applying a DC signal of 10mA & 1.5V to obtain bandwidth and pattern reconfigurability. The typical activation mechanism of the PIN diodes have been explained in details in our previous works [20], [21].

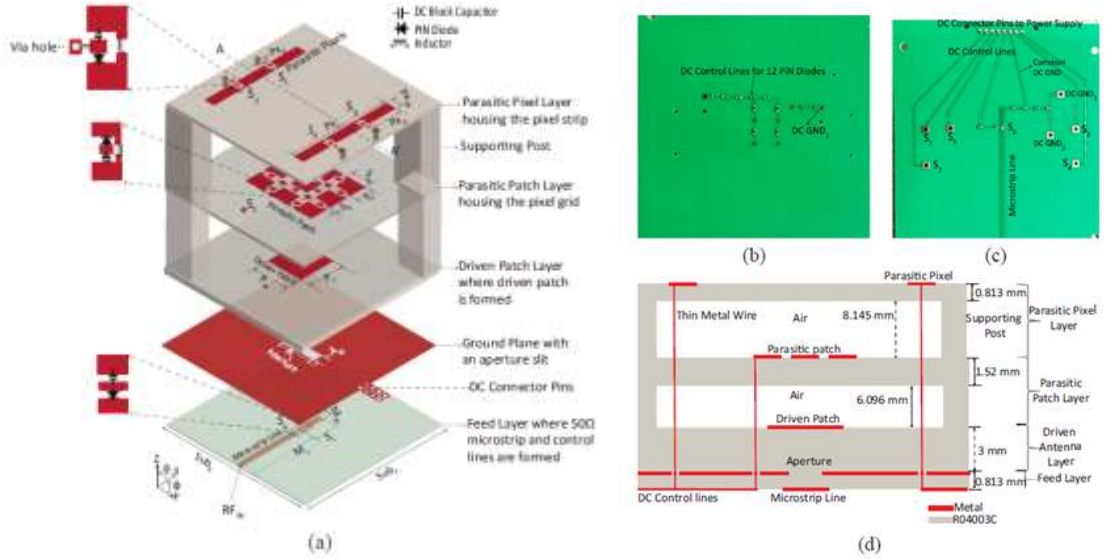

Fig. 1: (a) 3D exploded view of the RA, photograph of bottom face of the (b) parasitic patch layer and (c) feed layer, and (d) AA′ plane cross section of the RA.

As shown in Fig. 1(b), the dc controls for the 12 PIN diodes, which are needed to inter connect the pixels in the parasitic patch layer, have been distributed from one dc control line to reduce the complexity. The DC control lines are formed on the bottom surface of the feed layer underneath the ground plane (see Fig.1(c)). This structure provides shielding between control lines and radiating components thereby minimizing the EM coupling between them, which in turn eliminates the RF losses. Thin metal wires that run through all the layers, as shown in Fig.1(d), have been used to connect the DC control lines to the PIN diodes on the top surfaces of the parasitic patch and pixel layers. An electromagnetic (EM) full-wave analysis tool [22] was used to determine the geometrical dimensions of the overall structure and surface mount device (SMD) component values resulting in the desired impedance bandwidth variability and beam steering capabilities. The critical design parameters and the manufacturer details of the SMD components are provided in Tables 1 and 2.

TABLE 1: *Critical Design Parameters (in mm)*

S_X , S_Y	(6.4,6.4)	Sub_X, Sub_Y	(90,90)	P_W, P_L	(18,18)
P_{xw}	3	M_w	1.82	M_L	52.85
S_L	8.65	S_D	1	P_{xL}	48
A_L, A_W	(16,0.8)	P_{xs}	15	P_{xG}	1.5

TABLE 2: *Lumped Components values and self resonant frequencies(SRF) used in RA*

Component Type	Model	Value	SRF
PIN Diode	MA4AGFCP910	N/A	N/A
RF Choke	0603HP–39NXJLU	39 nH	3.5GHz
DC grounding inductor	0402HP–12NXGLU	12 nH	3.5GHz
DC block capacitor	GJM1555C1H1R3BB01D	1.3 pF	N/A
Bipolar Junction Transistor (BJT)	2N3904	N/A	N/A
Resistor (R1)	N/A	9.83 KΩ	N/A
Resistor (R2)	N/A	50.7 KΩ	N/A
Resistor (R3)	N/A	38 Ω	N/A

2.2 Working Mechanism

Bandwidth reconfigurability in the presented RA is obtained using multiple resonance technique [23]–[25]. A driven patch mutually couples to a slightly larger parasitic patch (parasitic patch layer), which has been pixelated into a grid of 3×3 metallic pixels. The effective electrical size of the parasitic patch can be increased/decreased by turning ON/OFF the interconnecting PIN diodes. By turning all the switches ON results in broad bandwidth, while keeping all switches in OFF state results in narrow bandwidth operation. The input impedance matching for broad and narrow bandwidth operations is accomplished by turning OFF and ON the single switch on the microstrip feed line, respectively. The parasitic layer housing two pixel strips is placed .16λ (at 3.5 GHz) above the driven antenna layer. The beam steering is accomplished by coupling the EM energy from driven and parasitic patch layers to parasitic pixel layer [26], [27]. Yagi-Uda principle [28]–[31] can be used to explain the beam-steering property of the this RA. The reconfigurable pixel strips act as reflector/director when their effective electrical lengths are changed by turning ON/OFF the interconnecting PIN diodes, and thus beam steering is obtained. The switches' status in obtaining the bandwidth and beam steering modes are given in Table 3.

TABLE 3: Switch Configurations for desired modes of operation (1=ON,0=OFF, BW=Bandwidth,(θ, φ)indicate peak gain direction)

Modes	θ	ϕ	BW(MHz)	S1	S2	S3	S4	S5	S6
1	0^0	0^0	200	0	0	0	0	0	1
2	30^0	0^0	200	0	0	1	1	0	1
3	-30^0	0^0	200	1	1	0	0	0	1
4	0^0	0^0	800	0	0	0	0	1	0
5	30^0	0^0	800	0	0	1	1	1	0
6	-30^0	0^0	800	1	1	0	0	1	0

3. Measurement and Simulation Results

3.1 Impedance and Pattern Characterization

A prototype RA was fabricated using standard printed circuit board fabrication processes and characterized to validate the simulation results. PIN diode switches are numbered in Figs. 1(a) and 1(c), as $S_i(i = 1 \ldots 6)$ to identify the switch status for each mode. The switch configuration and associated modes of operation are shown in Table 3.$S_i(i = 1, 2, 3, 4)$ are the switches integrated on parasitic pixel layer. $S5$ represents the twelve PIN diodes used in parasitic patch layer, as these switches are either all ON or all OFF states. $S6$ is the switch integrated on microstrip feed line. The maximum realized gain is $\sim 8dB$ for broadside, and $\sim 9dB$ for steered directions.

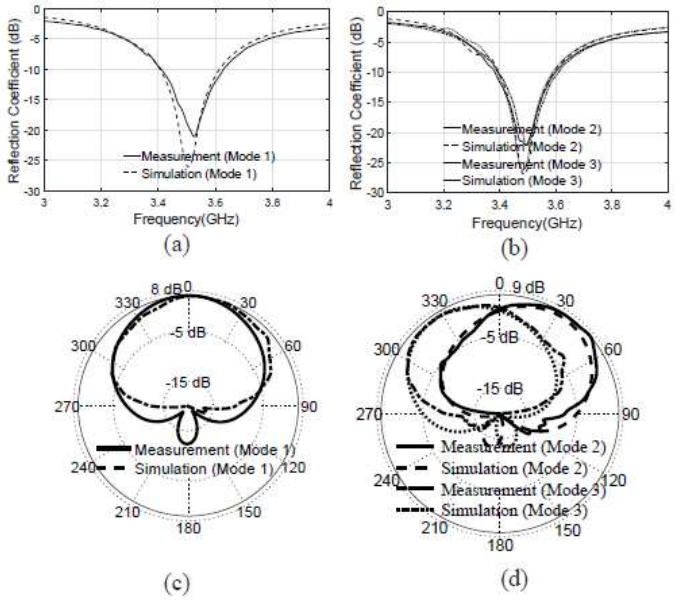

Fig. 2: Simulated and measured reflection coefficients of the RA for (a) mode 1 and (b) modes 2,3, and realized gain patterns for (c) mode 1 and (d)modes 2,3

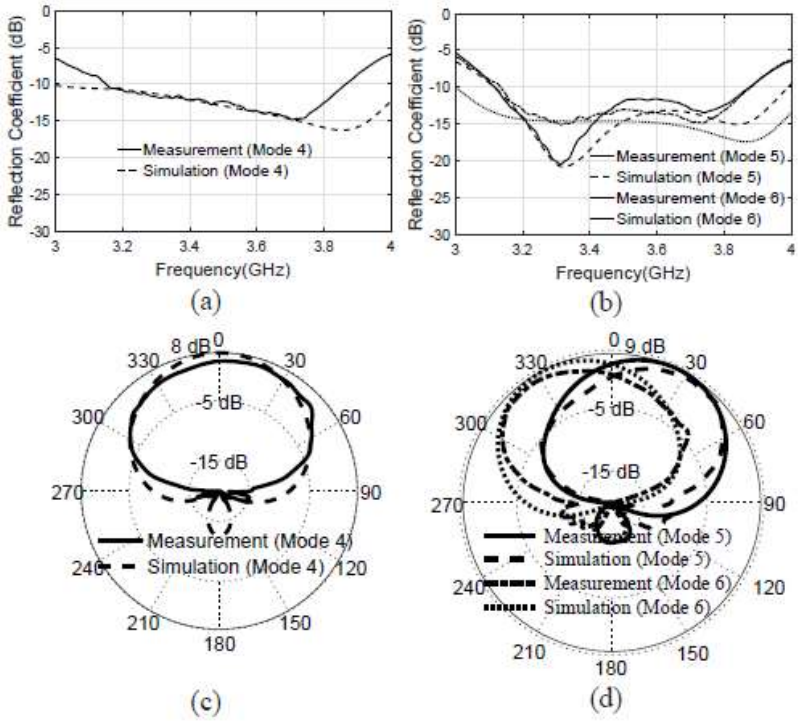

Fig. 3: Simulated and measured reflection coefficients of the RA for

(a) mode 4, (b) mode 5,6, and realized gain patterns for (c) mode 4, and (d) mode 5,6

(b)

4. Conclusion and Future Works

A parasitic layer based reconfigurable antenna (RA) targeting sub-6 GHz spectrum sharing applications, which is capable of dynamically changing its impedance bandwidths between narrow and broad frequency bands (3.4-3.6GHz & 3.1-3.9GHz) and concurrently steering its main radiation beam into three different directions (i.e $\theta \in \{-30^{\circ}, 0^{\circ}, 30^{\circ}\}$ for $\varphi \in \{0^{\circ}\}$) has been designed, manufactured and characterized. Reflection coefficient and radiation pattern results obtained

from measurements agreed well with the simulated results indicating an average maximum gain of around 9 dB for all modes of operations. As the RA technology starts finding practical applications in todays and future transceiver systems, i.e., fifth generation (5G) new radio, the characterizations of RAs in terms of system level parameters such as error vector magnitude (EVM) and passive intermodulation product (PIM) become important. The use of RF PIN diode switches in the presented RA causes small degradation in EVM performance as compared to passive horn antenna. For all six modes of operations, the EVM performances was good, where the measured EVMs were less than -25 dBm for an input power of 30 dBm.

References

[1] L. Ge and K. M. Luk, "Band-reconfigurable unidirectional antenna: A simple, efficient magneto-electric antenna for cognitive radio applica- tions." *IEEE Antennas and Propagation Magazine*, vol. 58, no. 2, pp. 18–27, 2016.

[2] S. Bhattarai, J.-M. J. Park, B. Gao, K. Bian, and W. Lehr, "An overview of dynamic spectrum sharing: Ongoing initiatives, challenges, and a roadmap for future research," *IEEE Transactions on Cognitive Communications and Networking*, vol. 2, no. 2, pp. 110–128, 2016.

[3] F. Hu, B. Chen, and K. Zhu, "Full spectrum sharing in cognitive radio networks toward 5g: A survey," *IEEE Access*, vol. PP, no. 99, pp. 1–1, 2018.

[4] B. P. Chacko, G. Augustin, and T. A. Denidni, "Electronically reconfi- gurable uniplanar antenna with polarization diversity for cognitive radio applications," *IEEE Antennas and Wireless Propagation Letters*, vol. 14, pp. 213–216, 2015.

[5] A. Goldsmith, S. A. Jafar, I. Maric, and S. Srinivasa, "Breaking spectrum gridlock with cognitive radios: An information theoretic perspective," *Proceedings of the IEEE*, vol. 97, no. 5, pp. 894–914, 2009.

[6] Y. Tawk, J. Costantine, and C. Christodoulou, "Cognitive-radio and antenna functionalities: A tutorial [wireless corner]," *IEEE Antennas and Propagation Magazine*, vol. 56, no. 1, pp. 231–243, 2014.

[7] R. Caromi, Y. Xin, and L. Lai, "Fast multiband spectrum scanning for cognitive radio systems," *IEEE Transactions on Communications*, vol. 61, no. 1, pp. 63–75, 2013.

[8] E. Erfani, J. Nourinia, C. Ghobadi, M. Niroo-Jazi, and T. A. Denidni, "Design and implementation of an integrated uwb/reconfigurable-slot antenna for cognitive radio applications," *IEEE Antennas and Wireless Propagation Letters*, vol. 11, pp. 77–80, 2012.

[9] E. Ebrahimi, J. R. Kelly, and P. S. Hall, "Integrated wide-narrowband antenna for multi-standard radio," *IEEE transactions on antennas and propagation*, vol. 59, no. 7, pp. 2628–2635, 2011.

[10] Y. Tawk and C. Christodoulou, "A new reconfigurable antenna design for cognitive radio," *IEEE Antennas and wireless propagation letters*, vol. 8, pp. 1378–1381, 2009.

[11] Z. Liu, K. Boyle, J. Krogerus, M. de Jongh, K. Reimann, R. Kaunisto, and J. Ollikainen, "Mems-switched, frequency-tunable hybrid slot/pifa antenna," *IEEE Antennas and Wireless Propagation Letters*, vol. 8, pp. 311–314, 2009.

[12] M. Hamid, P. Gardner, P. S. Hall, and F. Ghanem, "Switched-band vivaldi antenna," *IEEE transactions on antennas and propagation*, vol. 59, no. 5, pp. 1472–1480, 2011.

[13] B. Cetiner, H. Jafarkhani, J.-Y. Qian, H. J. Yoo, A. Grau, and F. De Fla- viis, "Multifunctional reconfigurable MEMS integrated antennas for adaptive MIMO systems," *IEEE Communications Magazine*, vol. 42, no. 12, pp. 62–70, 2004.

[14] F. A. Miranda, C. H. Mueller, and M. A. B. Meador, "Aerogel antennas communications study using error vector magnitude measurements," in *2014 IEEE Antennas and Propagation Society International Symposium (APSURSI)*, July 2014, pp. 1149–1150.

[15] G. H. Huff, N. Soldner, W. D. Palmer, and J. T. Bernhard, "Study of error vector magnitude patterns (evrp) for a transmit/receive pair of microstrip patch antennas," in *2006 IEEE Antennas and Propagation Society International Symposium*, July 2006, pp. 449–452.

[16] J. R. Wilkerson, I. M. Kilgore, K. G. Gard, and M. B. Steer, "Passive intermodulation distortion in antennas," *IEEE Transactions on Antennas and Propagation*, vol. 63, no. 2, pp. 474–482, Feb 2015.

[17] D. Wu, Y. Xie, Y. Kuang, and L. Niu, "Prediction of passive intermodu- lation on mesh reflector antenna using collaborative simulation: Multi- scale equivalent method and nonlinear model," IEEE Transactions on Antennas and Propagation, vol. PP, no. 99, pp. 1–1, 2017.

[18] D. M. Pozar, "Microstrip antenna aperture-coupled to a microstripline,"Electronics Letters, vol. 21, no. 2, pp. 49–50, January 1985.

[19] P. Sullivan and D. Schaubert, "Analysis of an aperture coupled microstrip antenna," IEEE Transactions on Antennas and Propagation, vol. 34, no. 8, pp. 977–984, Aug 1986.

[20] Z. Li, E. Ahmed, A. M. Eltawil, and B. A. Cetiner, "A beam-steering reconfigurable antenna for wlan applications," IEEE Transactions on Antennas and Propagation, vol. 63, no. 1, pp. 24–32, Jan 2015.

[21] D. Rodrigo, J. Romeu, B. A. Cetiner, and L. Jofre, "Pixel reconfigurable antennas: Towards low-complexity full reconfiguration," in 2016 10th European Conference on Antennas and Propagation (EuCAP), April 2016, pp. 1–5.

[22] HFSS, "Ansoft corp., pittsburgh, pa," 2015.

[23] P. Hall, C. Wood, and C. Garrett, "Wide bandwidth microstrip antennas for circuit integration," Electronics Letters, vol. 15, no. 15, pp. 458–460, 1979.

[24] J.-F. Zurcher, "The ssfip: A global concept for high-performance bro- adband planar antennas," Electronics Letters, vol. 24, no. 23, pp. 1433– 1435, 1988.

[25] F. Croq and D. M. Pozar, "Millimeter-wave design of wide-band aperture-coupled stacked microstrip antennas," IEEE Transactions on antennas and propagation, vol. 39, no. 12, pp. 1770–1776, 1991.

[26] X. Yuan, Z. Li, D. Rodrigo, H. S. Mopidevi, O. Kaynar, L. Jofre, anB. A. Cetiner, "A parasitic layer-based reconfigurable antenna design by multi-objective optimization," IEEE Transactions on Antennas and Propagation, vol. 60, no. 6, pp. 2690–2701, June 2012.

[27] D.Rodrigo, B. A. Cetiner, and L. Jofre, "Frequency, radiation pattern and polarization reconfigurable antenna using a parasitic pixel layer," IEEE Transactions on Antennas and Propagation, vol. 62, no. 6, pp. 3422–3427, June 2014.

[28] S. Uda, "Wireless beam of short electric waves," J. IEE, pp. 273–282, 1926.

[29] H.Yagi, "Beam transmission of ultra short waves," Proceedings of the Institute of Radio Engineers, vol. 16, no. 6, pp. 715–740, 1928.

[30] J. Huang, "Planar microstrip yagi array antenna," in *Antennas and Propagation Society International Symposium, 1989. AP-S. Digest*. IEEE,

[31] *D. Rodrigo, L. Jofre, and B. A. Cetiner, "Circular beam-steering reconfigurable antenna with liquid metal parasitics," IEEE Transactions on Antennas and Propagation, vol. 60, no. 4, pp. 1796–1802, April* 2012.